DOI: 10.1002/chem.200801466

Construction of Giant Porphyrin Macrorings Self-Assembled from Thiophenylene-Linked Bisporphyrins for Light-Harvesting Antennae

Kaori Fujisawa,[a] Akiharu Satake,*[a] Shun Hirota,[a] and Yoshiaki Kobuke*[a, b]

Abstract: As a model of bacterial photosynthetic light-harvesting antenna, a large number of porphyrin units were organized into barrel-shaped macrorings. Two imidazolylporphyrinatozinc(II) molecules were linked through either unsubstituted thiophenes or 3,4-dioctylthiophenes **1a** and **1b**, respectively. These structures were spontaneously organized by complementary coordination of the imidazolyl to zinc and produced a series of self-assembled fluorescent polygonal macrorings under high dilution conditions. The ring size increased compared with previous *m*-phenylene examples. The size distribution was also controlled by the presence of octyl substituents. A wide distribution of macrorings from 7- to >15-mer was obtained from **1a**, whereas macrorings ranging from 7- to 11-mer with a maximum population focused at the 8-mer were formed with **1b**. The size distribution was governed by competition between entropy-favored, smaller-ring formation and the enthalpy-favored, less-strained larger macroring. The UV/Vis spectra showed a gradual redshift for the larger rings reflecting an increase in the transition dipole interactions.

Keywords: coordination modes · cyclization · photosynthesis · porphyrinoids · self-assembly

Introduction

Photosynthetic purple bacteria have developed the efficient light-harvesting antenna systems[1–3] LH1[4,5] and LH2.[6] In pigment array B850 of the LH2 complex, eighteen bacteriochlorophylls (Bchls) are arranged in a slipped cofacial barrel structure supported by the protein matrix. Due to the close packing of the neighboring Bchl units, the absorption maximum of the lowest excitation band of B850 is redshifted from 800 nm, which is the λ_{max} of the monomeric Bchl unit. The absorption band of an even larger macroring of B870 (LH1) is shifted further to 870 nm by stronger exciton interactions. This energy-cascade system allows efficient harvesting of light energy to the reaction center. The ring structure without any terminals is a key for intra- and inter-ring energy migration by their degenerate energy levels.[7–9]

Construction of such antenna systems has long been a challenging target in view of their importance in biological energy transformation events. Porphyrin-based LH antennae have occupied a central position in these efforts because of their close similarity to the structural and photophysical properties of chlorophylls. Various covalently[10,11] and non-covalently[12–17] linked multiporphyrin systems have been constructed, and extensively reviewed.[18–29] In the preparation of macrorings, the intramolecular cyclization of the linear oligomeric species is important for suppressing polymer formation. Template-assisted coupling reactions have successfully afforded porphyrin macrorings,[30–37] whereas other investigations have employed coupling reactions[38–42] and self-assemblies by using coordination bonds[43,44] under high dilution conditions.

We have developed a supramolecular methodology for macroring formation by using complementary coordination of two terminal imidazolylporphyrinatozinc(II) units connected through an appropriate linker under dilute conditions. Coordination equilibrium leads to the exclusive formation of macrorings without production of linear byproducts. When a *m*-phenylene unit was used as the linker, pen-

[a] K. Fujisawa, Dr. A. Satake, Prof. Dr. S. Hirota, Prof. Dr. Y. Kobuke
Graduate School of Materials Science
Nara Institute of Science and Technology (NAIST)
Takayama 8916-5, Ikoma, Nara 630-0192 (Japan)
Fax: (+81) 743-72-6119
E-mail: satake@ms.naist.jp

[b] Prof. Dr. Y. Kobuke
Institute of Advanced Energy
Kyoto University
Gokasho, Uji 611-0011 (Japan)
Fax: (+81) 774-38-4577
E-mail: kobuke@iae.kyoto-u.ac.jp

Supporting information for this article is available on the WWW under http://dx.doi.org/10.1002/chem200801466.

tagonal and hexagonal macrorings were obtained in an almost 1:1 mixture.[45,46] Interestingly, the hexagonal macrorings showed faster excitation energy hopping (EEH) rates than the pentagonal structures.[47] The result suggested the importance of the orientation factor of linker-separated chromophore components in determining the EEH rates and encouraged us to prepare larger macrorings.

Toward the noncovalent approach, only two examples of the preparation of polygonal porphyrin rings larger than a hexagon have been reported.[48,49] Unfortunately, these structures were nonfluorescent because cobalt–porphyrin[48] was used or ferrocene[49] was directly connected to the porphyrin. Herein, we explored the use of a five-membered aromatic thiophene as the linker between bis(imidazolylporphyrinatozinc(II)) molecules for making larger macrorings with enlarged internal angles. Bisporphyrins **1a** and **1b** were designed with the two porphyrin units connected through thiophene as the 2,5-substituents. 3,4-Substituents were introduced into the thiophene of **1b** to control the ring size by modulating the internal angle of the porphyrins.

Results

Synthesis of unit porphyrins: The synthetic schemes for **8a** and **8b** are shown in Scheme 1. Condensation of dipyrromethane **2** (2.0 equiv), monoacetal-protected thiophene-2,5-dicarboxaldehyde **3** (1.5 equiv), and *N*-methylimidazolcarboxaldehyde **4** (1.0 equiv) in the presence of trifluoroacetic acid gave acetal-protected thiophenylporphyrins **5a** and **5b**. Acetal deprotection afforded **6a** and **6b** in yields of 5 and 4%, respectively, based on **4** and the second condensation was then carried out by stepwise addition of dipyrromethane **2** and aldehyde **4**. After neutralization with triethylamine followed by oxidation with chloranil, compounds **8a** and **8b** were obtained. Pure **8a** was isolated by a combination of SiO_2 and gel permeation chromatographies (GPC) in a yield of 10% based on **6a**. Similarly, bisporphyrin **8b** was obtained in a yield of 6.5% based on **6b**.

^{1}H NMR spectra of **8a** (Figure 1a) and **8b** (Figure 1b) revealed only one peak for **8a** corresponding to a *N*-methyl signal at $\delta = 3.44$ ppm, and no atropisomer was observed. In the case of dioctyl-substituted porphyrin **8b**, however, three *N*-methyl signals were observed at $\delta = 3.427$, 3.422, and 3.415 ppm, suggesting the presence of atropisomers (*syn-anti* isomers; Figure 1d). These results indicate that the porphyrin moieties for unsubstituted thiophenes rotate around the axis of the thiophene–porphyrin bond on the NMR spectroscopy timescale, but no rotation occurs with the dioctyl variant. Similarly, the ^{1}H NMR spectrum for **6b** showed the presence of *syn-anti* isomers.

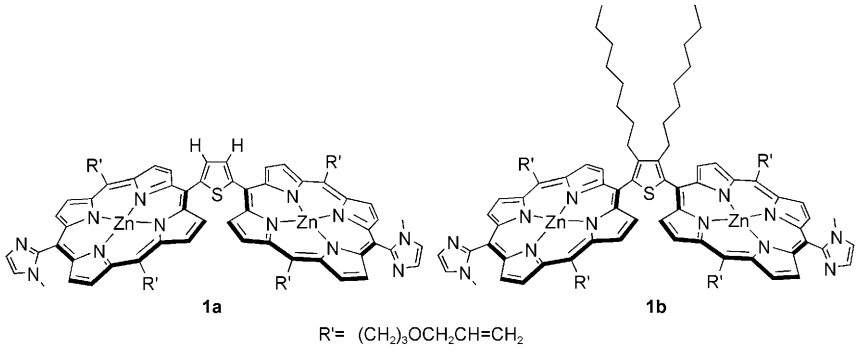

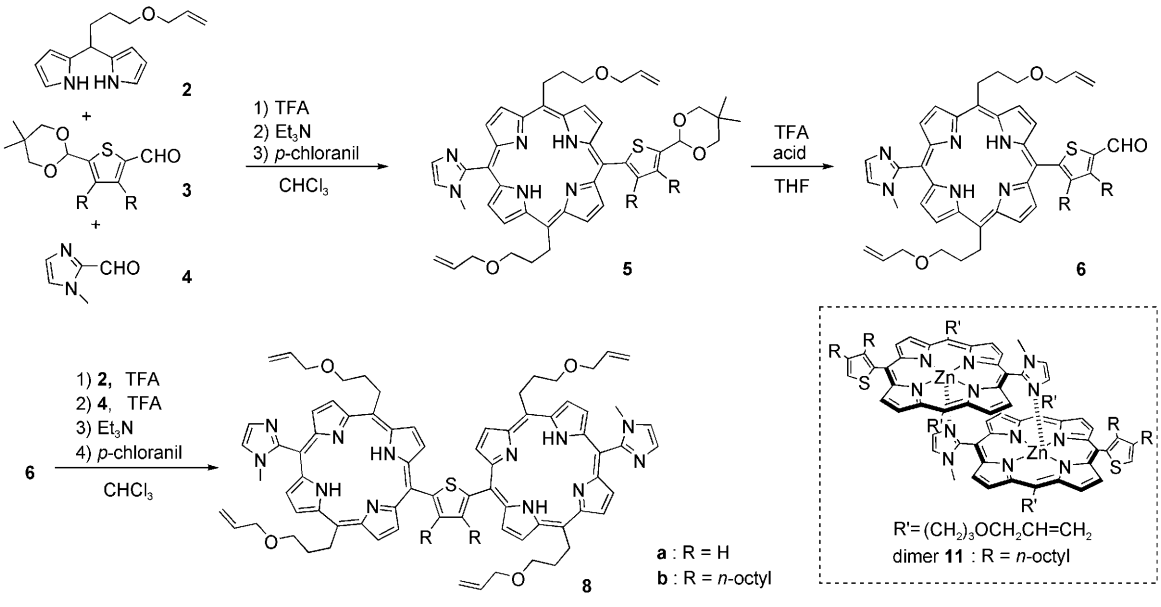

Scheme 1. Synthesis of thiophenylene-linked bisporphyrin.

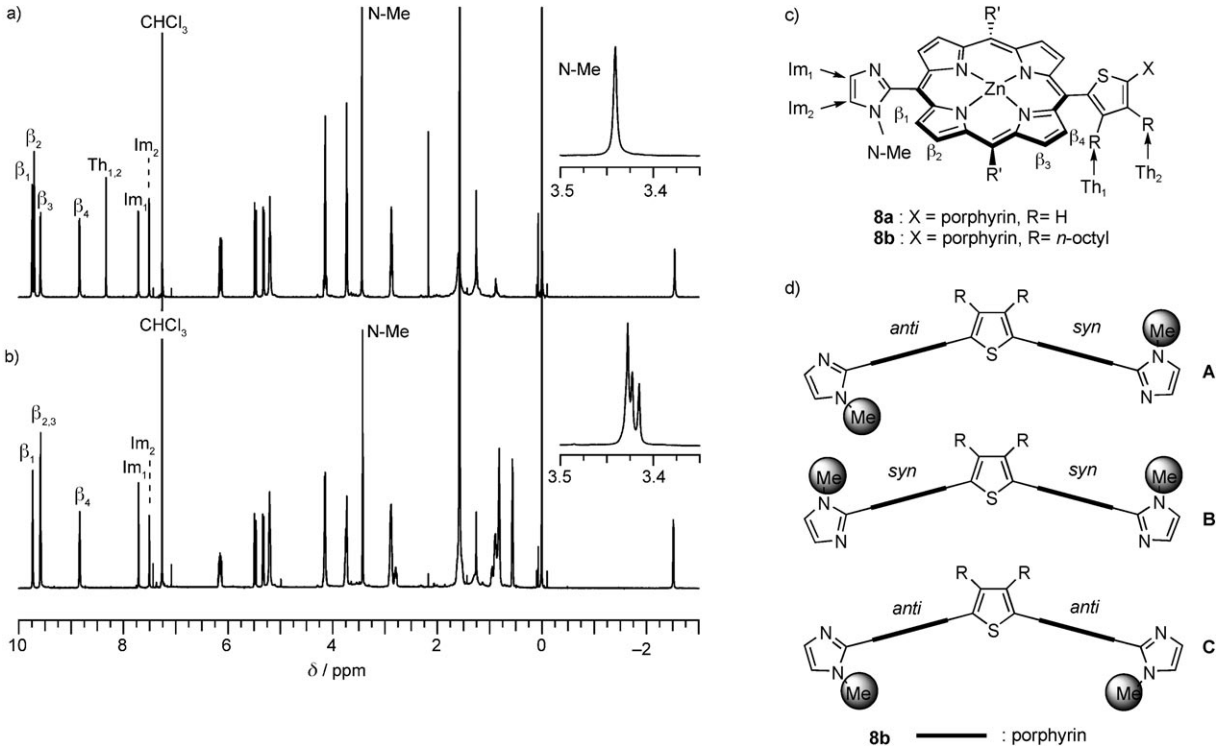

Figure 1. ^{1}H NMR (600 MHz) spectra of a) **8a** and b) **8b** in $CDCl_3$ at RT. The inset shows an enlargement of *N*-methyl part. The proton assignments (c) and atropisomers in **8b** (d; **A**: *anti-syn*, **B**: *syn-syn*, **C**: *anti-anti*) are also shown.

Ring formation from 1a and 1b: Fundamental procedures for ring formation based on strong complementary coordination of imidazolyl to zinc have been established in our previous studies.[45,46,49–51] Thus, a dilute solution of bis(imidazolylporphyrinatozinc(II)) units linked through an appropriate spacer was prepared in chloroform containing a small amount of methanol or ethanol. After equilibrium was achieved, ring compounds were formed exclusively without linear polymeric materials. The ring size should depend on the internal angle between the two imidazolylporphyrinatozinc(II) units separated by the linker.

Zinc(II) ions were introduced into free-base bisporphyrins **8a** and **8b** to give **1a** and **1b**, respectively (Scheme 2). Complementary coordination spontaneously started to give the initial gel permeation chromatogram at $t=0$ (Figure 2). Then, each sample of **1a** or **1b** was diluted to 10 μM by the addition of chloroform containing 0.5% ethanol. In the case of **1b**, 1% methanol (v/v) was added to accelerate the reorganization. The solutions were warmed to 47 °C. In a typical GPC analysis of the progress of the reorganization for **1a** (Figure 2a), the initial peak maximum appeared at 8.4 min, corresponding to 52000 Da, as estimated from polystyrene standards. During the course of reorganization, the peak maxima shifted progressively to longer retention times corresponding to increasingly smaller molecular weights. After 2.5 h, the shift of the peak maximum became significantly slower, but the reorganization still proceeded, as determined by the small shift and sharpening of the peak. By 18 h, the progress had almost stopped at the retention time for the peak maximum at 11.3 min, corresponding to an apparent mass of 11000 Da; no further change was observed after 24 h, suggesting the final convergence (Figure 2a). For **1b**, the chromatogram after 18 h showed the peak at 11.7 min (Figure 2b), which was identical to that at 24 h and suggested that final convergence had been achieved. The observed behavior is common to the reorganization processes of other *m*-phenylene-linked bis(imidazolylporphyrinatozinc(II)) structures[45] and the converged compounds suggest macroring formation.[45,49,51,52] The whole reorganization processes may be illustrated as shown in Scheme 2.

Since coordination-organized supramolecules give only dissociated ionic species in the mass spectrum, the molecular weight must be obtained after covalent linking of coordination pairs through a ring-closing metathesis reaction[46] with the use of the Grubbs catalyst to produce the converged sample of **1b** (Scheme 3). In a MALDI-TOF mass spectrum acquired after the metathesis reaction of the crude converged samples, defined as C-$(\mathbf{1b})_{mix}$ to differentiate from samples before metathesis, N-$(\mathbf{1b})_{mix}$, 7- to 9-mers were observed as the major products with lesser peaks of 10- and 11-mer also observed (Figure 3a). Fractions 1–4 of the metathesis product, C-$(\mathbf{1b})_{mix}$, were isolated by recycling GPC using pyridine as the eluent (see Figure S1 in the Supporting Information, fractions 1–4). The mass spectra of fractions 1–4, which contained oligomers ranging from 7- to 10-mer, gave a series of peak maxima that agreed well with the cal-

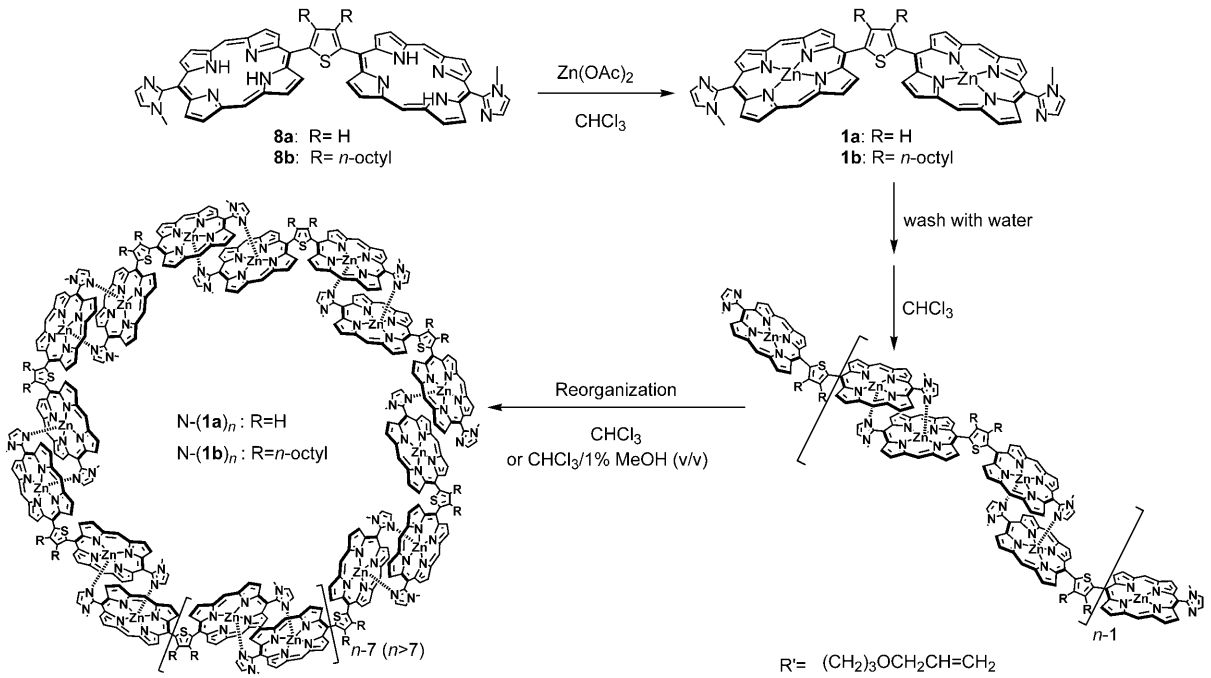

Scheme 2. Synthesis, self-assembly, and reorganization of **1a** and **1b**. Allyloxy propyl groups (R′) at the *meso*-position are omitted.

culated[53] molecular weights ($[M+H]^+$) for C-(**1b**)$_n$ within an error range of ± 2 Da (Figure 3b–e). The series of compounds thus proved to be composed of macroring structures.

The size distribution of a mixture before metathesis (N-(**1b**)$_{mix}$) yields important information about the effect of the internal angle on the ring size. The distribution of C-(**1b**)$_{mix}$ may not be precise because although the metathesis reaction proceeds very well it is not quantitative. Therefore, data from the N-(**1b**)$_{mix}$, showing two peaks and two shoulders in twice-recycled GPC, were separated into fractions a–d. Fractions a–d were assigned as 7- to 10-mers by comparing the retention times with the calibration line prepared by C-(**1b**)$_{7–10}$ (Figure 4). Then, the recycling GPC chart of N-(**1b**)$_{mix}$ was deconvoluted (Figure 5a). The peaks were approximated by a Gaussian function to give 7- to 11-mers as major macrorings with a maximum at 8-mer: 7-mer $=(27\pm 2)$, 8-mer $=(36\pm 2)$, 9-mer $=(18\pm 1)$, 10-mer $=(11\pm 2)$, larger than 11-mer $=(7\pm 3)\,\%$. We also tried to estimate the ring sizes and the distribution of the converged sample of **1a**, N-(**1a**)$_{mix}$ (Figure 5b). At least ten peaks were partially separated, with significant overlapping of the other peaks. Therefore, the section of the chromatogram showing partial separation (retention time ≥ 130 min) was deconvoluted, and the higher oligomer section (40 %) was ignored. Each peak was assigned as 7- to >15-mer by comparing the retention times with the calibration line prepared by C-(**1a**)$_{9–11}$. When evaluated in this manner, the size distribution of N-(**1a**)$_{7–15}$ was much wider: 7-mer $=(12\pm 1)$, 8-mer $=(12\pm 1)$, 9-mer $=(13\pm 1)$, 10-mer $=(12\pm 1)$, 11-mer $=(11\pm 1)$, 12-mer $=(10\pm 1)$, 13-mer $=(9\pm 1)$, 14-mer $=(8\pm 1)$, larger than 15-mer $=(10\pm 2)\,\%$.

UV/Vis absorption and fluorescence spectra: The UV/Vis absorption spectra of a series of rings, C-(**1b**)$_{7–10}$, were measured in pyridine (Figure 6). Even in strongly coordinating solvents, such as pyridine, covalently linked macrorings retain their cyclic structures.[46,47,51,53] The peak maxima of the split Soret bands at longer wavelengths were gradually redshifted in the order 7-<8-<9-<10-mer (insets of Figure 6).

The fluorescence quantum yields (Φ_F) of N-(**1b**)$_{7–10}$ in chloroform and C-(**1b**)$_{7–9}$ in pyridine showed similar values (0.015 ± 0.008), which were about half of that of the unit dimer **11**.

Discussion

Macroring formation: If monomeric terminal units exist in the converged N-(**1b**)$_{mix}$, the size distribution of the monomers in N-(**1b**)$_{mix}$ must depend on the concentration.[48,54] We analyzed the samples of N-(**1b**)$_{mix}$ by GPC at two different concentrations (80 and 10 μM), but obtained almost identical elution curves. More decisively, the mass spectra obtained after the covalent linking gave the correct molecular weights[53] calculated based on ring structures (Figure 3a–d). We therefore concluded that converged N-(**1b**)$_n$ and its covalently linked analogue C-(**1b**)$_n$ are cyclic structures.[46,49,51]

Rotation around the axis of the thiophene–porphyrin bond: Observation of atropisomers in **6b** and **8b** indicated that *syn-anti* isomerization was slowed by the introduction of octyl groups. Based on variable-temperature NMR spectroscopy studies performed in $(CDCl_2)_2$, the rate constant (k_r)

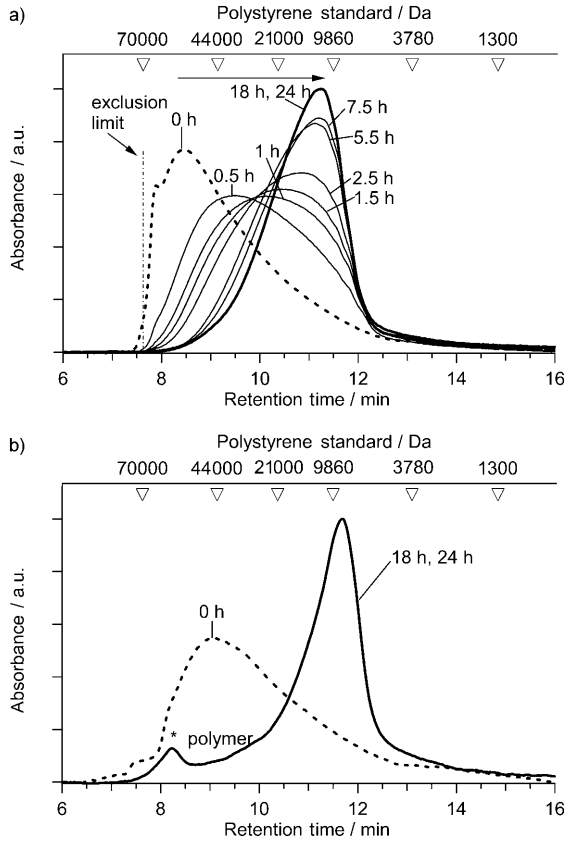

Figure 2. GPC analyses of the reorganization process. a) **1a** in chloroform: samples of **1a** at various time intervals, from left to right, 0 (dotted line), 0.5, 1, 1.5, 2.5, 5.5, 7.5, 18 (solid bold line), and 24 h (solid line). b) For **1b** in chloroform with 1% (v/v) methanol: 0 h (dotted line), after 18 h (solid bold line). Open triangles at the tops of graphs represent the maximum peak position of polystyrene standards. Conditions: column: JAIGEL 3H-A (polystyrene gel, diameter = 8 mm, length = 50 cm, exclusion limit = 70000 Da); eluent, $CHCl_3$/0.05% Et_3N.

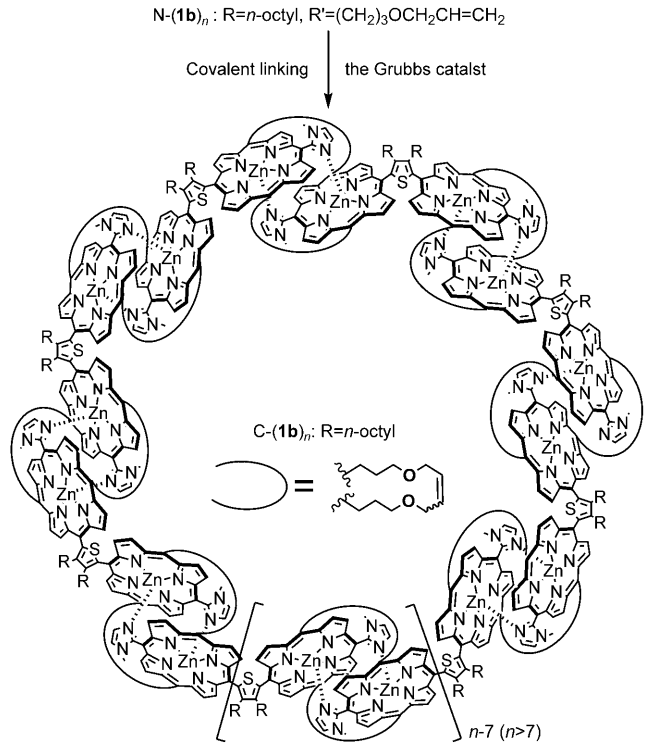

Scheme 3. Covalent linking of N-(**1b**)$_n$. Allyloxy propyl groups (R′) at the *meso*-position.

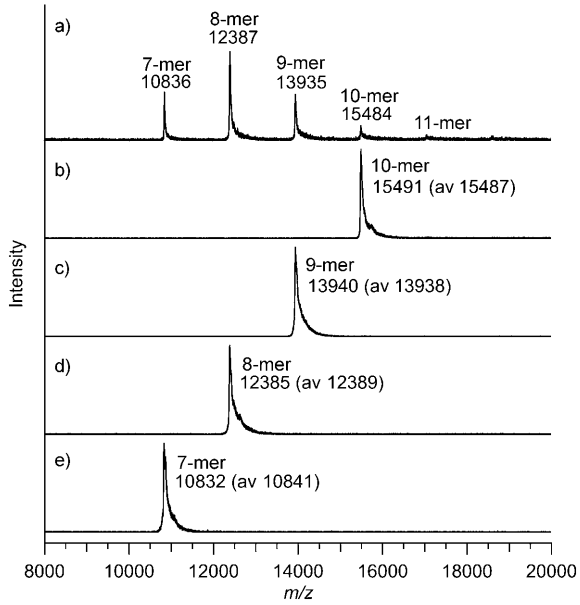

Figure 3. Mass spectra of a) C-(**1b**)$_{mix}$ and fractions 1 (b), 2 (c), 3 (d), and 4 (e); values indicate observed maximum peak number.

and the activation free energy ($\Delta G^{\ddagger}$) of *syn–anti* isomerization in **6b** were estimated (Figure S2 in the Supporting Information) to be $k_{r(323\,K)} = 12.0\ s^{-1}$ and $k_{r(383\,K)} = 28.0\ s^{-1}$, and $\Delta G^{\ddagger}_{323\,K} = 72.5\ kJ\,mol^{-1}$ and $\Delta G^{\ddagger}_{383\,K} = 83.8\ kJ\,mol^{-1}$, respectively. The $\Delta G^{\ddagger}_{298\,K}$ value of 67.9 kJ mol^{-1} obtained from the Eyring plot is slightly less than that of the *meso*-phenyl group in the substituted imidazolyl porphyrin ($\Delta G^{\ddagger}_{298\,K} = 71.1\ kJ\,mol^{-1}$). Since the rotational energy of the *meso*-imidazolyl group on the porphyrin is higher than that of the *meso*-phenyl group,[55] the rotation around the porphyrin–dioctylthiophenylene bond must account for the presence of atropisomers rather than rotation about the imidazolyl moiety. Consistent with this proposal, no atropisomer was observed for **6a** at 298 K, suggesting rapid rotation.

Although the conformational restriction was observed in the ^1H NMR spectrum of **8b** based on the following observations, rotation should occur under reorganization conditions. Atropisomers of **8b** could be detected as three spots on a silica gel TLC plate. When any one of the spots were isolated by column chromatography on SiO_2, the collected fraction showed three spots upon repeated TLC analysis, confirming that isomerization among atropisomers occurs after separation. Because reorganization of **1b** usually requires more than 10 h, the presence of atropisomerization does not introduce any barriers for ring formation.

With respect to slow rotation around the axis connecting the porphyrin and thiophene, structural isomers arise from

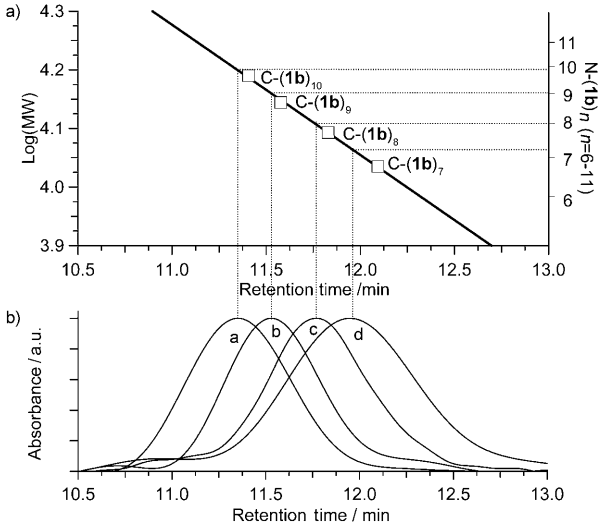

Figure 4. a) Logarithmic plots of the molecular weights against the retention time from Figure S1b in the Supporting Information. □: C-$(\mathbf{1b})_{7-10}$, ——: the calibration line for a series of C-$(\mathbf{1b})_n$. b) Analytical GPC chromatograms of fractions a–d of separated N-$(\mathbf{1b})_{mix}$. The conditions were the same as those given in Figure 2. Fractions a–d were assigned as the 7- to 10-mers by the calibration line given in (a).

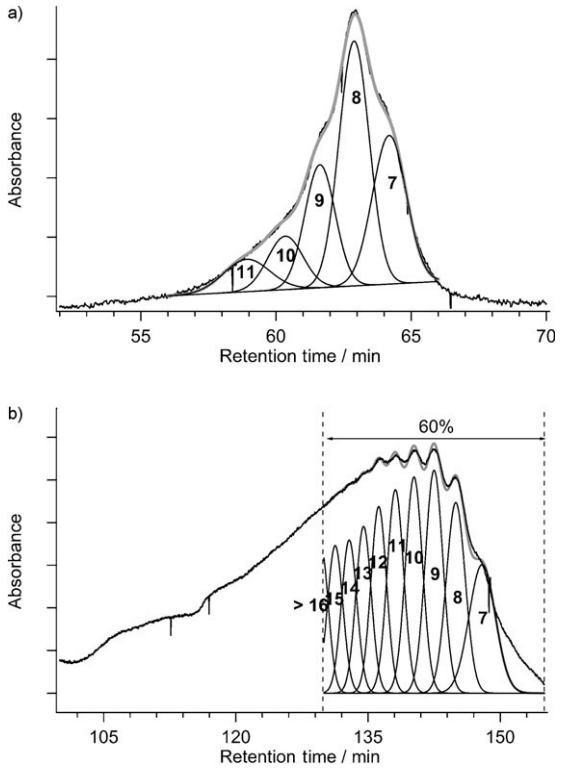

Figure 5. Deconvolution analyses of recycling GPC charts for a) N-$(\mathbf{1b})_{mix}$, b) N-$(\mathbf{1a})_{mix}$. Solid bold line: experimental data, solid line: deconvoluted peaks, grey line: sum of the deconvoluted peaks. In this analysis, 40% of the higher molecular weight polymer (>15-mer) was ignored.

out and in coordination.[55] Two of the possible eight geometrical isomers are depicted schematically for the 7-mer in Figure 7. Ring **D** only contains out-in (o-i) geometry, where-

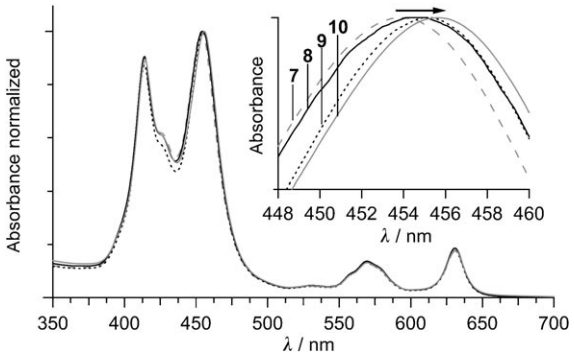

Figure 6. UV/Vis spectra of C-$(\mathbf{1b})_7$ (grey dashed line), C-$(\mathbf{1b})_8$ (solid line), C-$(\mathbf{1b})_9$ (dotted line), and C-$(\mathbf{1b})_{10}$ (grey line), in pyridine at RT. The inset shows an enlargement of the Soret band at longer wavelengths.

as ring **E** contains one in-out (i-o) geometry and is represented by i-o, o-i, o-i, o-i, o-i, o-i, and o-i, from the right-hand edge (Figure 7). These isomers could not be distinguished from each other by GPC analysis.

Size population of reorganized macrorings for 1a and 1b: Introduction of two octyl groups at thiophene β positions may significantly affect the molecular structure. Molecular orbital calculations (AM1)[56] showed that the torsional angles between porphyrin and thiophene are 64 and 54° for **1a**, but were 90 and 89° for **1b** (Figure S3 in the Supporting Information). The internal angles between two porphyrins were 154° for **1a** and 148° for **1b**. Introduction of two octyl groups induces not only an orthogonal conformation, but also a smaller internal angle. The internal angle of **1a** was decreased to 151° when two porphyrins were located orthogonally to the thiophene moiety. Thus, the internal angles may vary between 151 and 154° relative to the tilt motion and widen the distribution for **1a**. In addition, the internal angle difference between the cyclic *n*-mer and the *n*+1-mer decreases in larger polygons, and thus the stability differences become smaller. This factor would also contribute to the wider size distribution of the macroring N-$(\mathbf{1a})_{mix}$.

The calculated internal angle (148°) of the unit bisporphyrin **1b** suggests that the cyclic 11-mer is the macroring with the least steric strain. Experimentally, the distribution is shifted towards macrorings of smaller unit numbers. To obtain a quantitative understanding, Gibbs energy differences were evaluated for equilibria between the 8-mer and the cyclic *n*-mer [$n=7$, 9, and 11; Equilibria (a)–(c)].

$$8\text{-mer} \rightleftharpoons 7\text{-mer} \quad \text{(a)}$$

$$8\text{-mer} \rightleftharpoons 9\text{-mer} \quad \text{(b)}$$

$$8\text{-mer} \rightleftharpoons 11\text{-mer} \quad \text{(c)}$$

The enthalpy changes for the respective equilibrium of the 8-mer and cyclic *n*-mer were calculated from the heats of formation (H_f) by semi-empirical molecular orbital methods, AM1.[56,57] To facilitate the calculation, substituents on

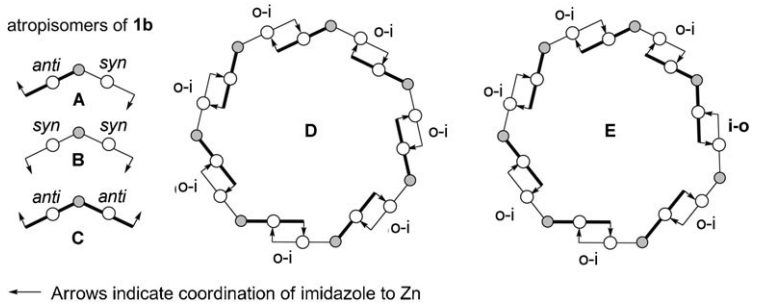

Figure 7. Two of eight possible macroring structures of C-$(\mathbf{1b})_7$. Ring **D** is composed of seven **A**'s and ring **E** is composed of five **A**'s, one **B**, and one **C**.

the porphyrin at the *meso*-positions and on the thiophenylene were replaced by protons and methyl groups, respectively. The entropy changes were estimated by using a model based on association for an aggregate of rigid particles.[58] The estimated thermodynamic parameters were listed in Table 1 and plotted in Figure 8 as a function of the internal angle of the *n*-mer. The entropy change per unit bisporphyrin from 8-mer to cyclic *n*-mer decreases almost linearly for larger macrorings and favors entropically smaller macrorings. On the other hand, smaller macrorings are disfavored enthalpically. Calculated Gibbs energies (8-mer ≤ 7-mer < 9-mer < 11-mer) of formation per unit bisporphyrin successfully reflected the experimental population of the macrorings (8-mer < 7-mer < 9-mer < 10-mer < 11-mer).

Table 1. Gibbs free energy change (ΔG) per unit porphyrin in Equilibria (a)–(c).

Equilibrium	ΔH [kcal mol]	$T\Delta S$[a] [kcal mol]	ΔG[b] [kcal mol^{-1}]
a	6.3	5.8	0.6
b	−2.0	−4.5	2.6
c	−3.2	−11.2	8.0

[a] $T = 320$ K. [b] $\Delta G = \Delta H - T\Delta S$.

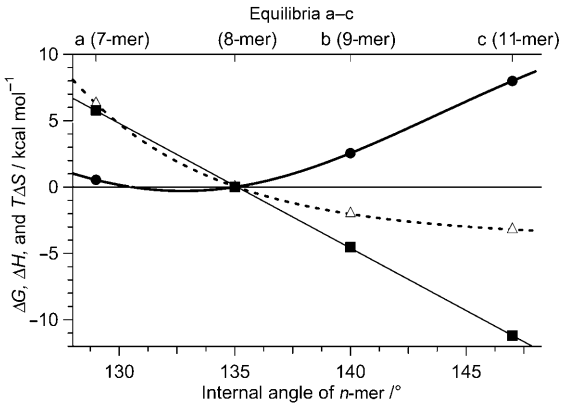

Figure 8. Approximate $T\Delta S$ (solid line, $T = 320$ K), ΔH (dotted line), and ΔG (bold line) changes from the 8-mer to the *n*-mer per coordination dimer for 7- to 11-mers as a function of the internal angle of the *n*-mer.

UV/Vis spectra: The origin of the split Soret bands in **1a**, **1b**, and the macrorings may be explained on the basis of excitonic coupling theory, in a manner similar to earlier studies.[59,60] The degenerated transition dipole moments are split as a result of slipped cofacial dimer formation. In Figure 6, the peak maxima of the longer Soret bands were systematically redshifted in the order of increased ring sizes. A similar tendency was observed for pentagonal and hexagonal macrocyclic porphyrins.[47,51,60] In the present case, a more generalized treatment may be required by including interactions among not only the neighboring porphyrins, but also with other component porphyrins in the macrorings.

Calculation of the interaction energies was undertaken as follows: A macroring was placed in the center of *x*–*y* coordinate. If the electric field of the input light comes from the *x*-axis direction, only the *x* component of each transition dipole interacts with the light. All of the transition dipoles, $\boldsymbol{m}_m$, are divided into *x* and *y* components, $\boldsymbol{m}_{mx}$ and $\boldsymbol{m}_{my}$ (see Figure S4, left in the Supporting Information). The total excitonic coupling energy for all of the porphyrins in each macroring can be calculated by using Equation (1).[59,61]

$$E = \sum_{n,m(m>n)} \frac{2\boldsymbol{m}_{mx}\boldsymbol{m}_{nx}\kappa_{mx,nx}}{\boldsymbol{R}^3_{mx,nx}} \quad (1)$$

in which $\boldsymbol{m}_{mx}$ and $\boldsymbol{m}_{nx}$ are the *x* components of the transition dipole moments of *m* and *n*th complementary dimer units, $\boldsymbol{R}_{mx,nx}$ is the center-to-center distance between $\boldsymbol{m}_{mx}$ and $\boldsymbol{m}_{nx}$, and $\kappa_{mx,nx}$ is the orientation factor of $\boldsymbol{m}_{mx}$ and $\boldsymbol{m}_{nx}$. It is defined by Equation (2) and Figure S4, right in the Supporting Information.

$$\kappa_{mx,nx} = 1 - 3\cos^2\theta \quad (2)$$

If the scalar of the transition dipoles, $|\boldsymbol{m}_m|$, is defined as m_0, the total coupling energies are expressed as shown in Table 2. The coupling energy increases with increasing ring size. Interestingly, the larger ring is associated with the larger coupling interactions. Faster rates of EEH for the hexagons rather than for the corresponding pentagons have

Table 2. The total excitonic coupling energy *E* in the 7- to 12-mer estimated from Equation (1).

Ring size (*n*-mer)	$E \times 10^6$ (m_o^2)
7	−1451
8	−1810
9	−1981
10	−2299
11	−2491
12	−2788

already been observed[47,51,60] and measurements of the EEH rates for a series of systematic ring variations of this study may extend this tendency. Further studies are ongoing.

Conclusion

Bis(imidazolylporphyrinatozinc(II)) compounds **1b** and **1a** linked through either 3,4-dioctylthiophenylene or unsubstituted 2,5-thiophenylene units were synthesized. They were linked by complementary coordination of imidazolyl to zinc and produced a series of self-assembled fluorescent polygonal macrorings larger than hexagons under the appropriate reorganization conditions. The macroring size was controlled by the internal angles between the two porphyrins linked through thiophenylene and also by the introduction of the octyl groups. The ring size distribution was rationalized by the balance between favorable entropy and enthalpic instability due to angle strain for the smaller rings. A very wide distribution of macrorings from 7- to >15-mer was obtained from unsubstituted bisporphyrin **1a**, whereas for **1b**, the macroring distribution was limited to 7- to 11-mer, with the maximum population centering at the 8-mer. After covalent linking of coordination pairs, cyclic 10-mer (C-(**1b**)$_{10}$), 9-mer (C-(**1b**)$_9$), 8-mer (C-(**1b**)$_8$), and 7-mer (C-(**1b**)$_7$) were isolated in a pure form through recycling GPC. In the UV/Vis spectra, the longer Soret bands in the polygonal macrorings were gradually redshifted as the ring size increased. This observation was supported by a gradual increase of the coupling interactions of porphyrin transition dipoles.[47,51]

Experimental Section

General: Analytical GPC was performed on a Hewlett-Packard HP1100 series instrument using a JAIGEL 3H-A column (Japan Analytical Industry, polystyrene gel, diameter = 8 mm, length = 50 cm, exclusion limit = 70000 Da, eluent: $CHCl_3$/0.05% Et_3N) or a Shimadzu LC workstation M10 equipped with an SPD-M10 AVP photodiode array detector using a Tosoh TSK-GEL G3000H$_{HR}$ column (polystyrene gel, exclusion limit = 60000 Da). Recycling GPC was carried out on a recycling GPC–HPLC system (Japan Analytical Industry, LC-908) connected with two series columns (JAIGEL 3HA, diameter = 20 mm, length = 60 cm × 2, polystyrene, exclusion limit = 70000 Da, eluent: $CHCl_3$/0.05% Et_3N), or two series columns of Tosoh TSK-GEL G3000H$_{HR}$ (polystyrene gel, exclusion limit = 60000 Da, eluent: pyridine). Column chromatography was performed using silica gel (silica gel 60N (spherical, neutral) 63–210 μm, KANTO) and aluminum oxide (aluminum oxide 90 active basic (0.063–0.200 mm), Merck). Preparative GPC was performed on a glass column (diameter = 1 cm, length = 100 cm) packed with Biobeads SX-3 (BioRad, polystyrene, exclusion limit = 2000 Da; flow rate: ca. 0.8 mL min^{-1}) using toluene as the eluent. MALDI-TOF mass spectra were measured on KRATOS AXIMA and Bruker autoflex II instruments with dithranol (Aldrich) or *trans*-2-[3-(4-*tert*-butylphenyl)-2-methyl-2-propenylidene]malononitrile (Fluka) as a matrix.

Synthesis of porphyrins: *meso*-(3-Allyloxypropyl)dipyrromethane **2**[53] and 1-methylimidazol-2-carboxaldehyde **4**[62] were synthesized according to reported procedures. Synthesis of 3,4-dioctylthiophene (**S1**), 3,4-dioctylthiophene-1-carbaldehyde (**S2**), 5-(5,5-dimethyl-[1,3]dioxan-2-yl)-3,4-dioctylthiophene (**S3**), compounds **3a**, **3b**, **5a**, **6a**, **6b**, **8a**, and **8b** are described in the Supporting Information.

2,5-Bis(15-*N*-methylimidazolylporphyrinatozinc(II))-3,4-dioctyl-thiophene (**1b**): A solution of zinc acetate dihydrate (4.0 mg, 18.2 μmol) in methanol (0.5 mL) was added to a solution of **8b** (2.1 mg, 1.4 μmol) in chloroform (1.0 mL). The mixture was stirred at RT for 3.5 h. Incorporation of the zinc(II) ion was confirmed by UV/Vis and fluorescence spectroscopies. A saturated aqueous solution of $NaHCO_3$ (1.0 mL) was added to the mixture. The organic layer was washed with water, dried over anhydrous Na_2SO_4, and evaporated to dryness. The residue was purified by reprecipitation from chloroform and *n*-hexane to afford **1b** (2.0 mg, 90.1%). The crude porphyrinatozinc(II) compounds were analyzed by GPC (Figure 2b, dotted line). The peak maximum appeared at 9.1 min, corresponding to 44000 Da estimated from polystyrene standard. MS (MALDI-TOF, dithranol): *m/z*: 1604.9 $[M+H]^+$ (Figure S18a).

2,5-Bis(15-*N*-methylimidazolylporphyrinatozinc(II))thiophene (**1a**): Compound **1a** was obtained according to a procedure similar to that for **1b** (3.6 mg, 81.5%). MS (MALDI-TOF, dithranol): *m/z*: 1380.8 $[M+H]^+$ (Figure S18b).

Reorganization of 1b: A solution of **1b** (0.8 mg, 0.49 μmol) in chloroform/1% MeOH (v/v; 50 mL) was kept at 47 °C in the dark. After 18 h, the solution was cooled to −40 °C, and then evaporated at 0 °C under reduced pressure (ca. 10 hPa) to give N-(**1b**)$_{mix}$ (Figure 2b). The solution was divided into several portions (less than 50 mL) and evaporated, since the use of larger volumes significantly changed the size distribution. The sample (N-(**1b**)$_{mix}$) was separated by recycling GPC (JAIGEL 3HA, eluent: chloroform/0.05% Et_3N) to give fractions a–d. The separated solutions were analyzed by analytical GPC (Figure 4b).

Reorganization of 1a: According to a procedure similar to that for **1b**, compound **1a** was reorganized by using a solution of **1a** (0.5 mg, 0.36 μmol) in chloroform containing 0.5% ethanol (36 mL) (Figure 2a). The sample (N-(**1a**)$_{mix}$) was separated by recycling GPC (JAIGEL 3HA, eluent: chloroform/0.05% Et_3N). The seven separated fractions were analyzed by analytical GPC.

Metathesis reaction of N-(1b)$_{mix}$: The ring-closing metathesis reaction was carried out for the reorganized sample (N-(**1b**)$_{mix}$) (1.4 mg, 0.88 μmol, in dichloromethane (10 μM)) by using the first generation Grubbs catalyst (0.72 mg, 0.88 μmol). The reaction progress was monitored by GPC analysis (Tosoh; eluent: pyridine). After 5 h the metathesized sample (C-(**1b**)$_{mix}$) was analyzed by MALDI-TOF mass spectrometry (Figure 3a). From the mixture of C-(**1b**)$_{mix}$, 7-, 8-, 9-, and 10-mer macrorings were isolated by recycling GPC with pyridine as the eluent using two series columns (Tosoh) (Figure S1 in the Supporting Information). The total amount of C-(**1b**)$_7$, C-(**1b**)$_8$, C-(**1b**)$_9$, and C-(**1b**)$_{10}$ was 0.5 mg. These samples were reanalyzed by analytical GPC (Figure S1b in the Supporting Information) to prepare the calibration line (Figure 4a). MS (MALDI-TOF, *trans*-2-[3-(4-*tert*-butylphenyl)-2-methyl-2-propenylidene]-malononitrile): *m/z*: 10832 (C-(**1b**)$_7$), 12385 (C-(**1b**)$_8$), 13940 (C-(**1b**)$_9$), 15491 (C-(**1b**)$_{10}$) $[M+H]^+$.

Estimation of macroring compositions from the recycling GPC chart of N-(1b)$_n$: The deconvolution analyses of GPC chromatograms were conducted with the Origin Pro 7 software (OriginLab) with the peak fitting module using the Gaussian function. The recycling GPC chart of N-(**1b**)$_n$ (Figure 5a) was analyzed by using the initial parameters in Table S1 in the Supporting Information. Five components (n = 7–11) were prepared as the initial set, their peak positions being adjusted manually to fit the observed peaks. Half-band widths of 7- to 11-mers were set as (1.5 ± 0.5) min. This analysis was carried out five times to give the following compositions: 7-mer = (27 ± 2), 8-mer = (36 ± 2), 9-mer = (18 ± 1), 10-mer = (11 ± 2), and larger than 11-mer = (7 ± 3)%. Similarly, deconvolution analysis of recycling GPC chart of N-(**1a**)$_n$ was carried out (Figure 5b). For this analysis higher oligomers (40% of the total) were ignored.

Estimated sum of interactions for all of the transition dipoles: To estimate the sum of interactions among all of the transition dipoles, a macroring was placed in the center of *x*–*y* coordinate. The numbers were posted to the transition dipoles clockwise as $\boldsymbol{m}_1$, $\boldsymbol{m}_2$, and so forth. All of the transition dipoles, $\boldsymbol{m}_m$, were divided into *x* and *y* components, $\boldsymbol{m}_{mx}$ and $\boldsymbol{m}_{my}$. The center-to-center distance between the *m* and *n*th transition dipoles was estimated mathematically by using the length of the bispor-

phyrin dimer (18.38 Å) determined by AM1 method. The total excitonic coupling energy for all of the porphyrins in each macroring was calculated by using Equations (1) and (2). The results are listed in Tables S3–S8 in the Supporting Information.

Acknowledgements

This work was supported by KAKENHI (20550098) (A.S.) from the Japan Society for the Promotion of Science (JSPS), and Kyoto-advanced nanotechnology network (A.S., Y.K.).

[1] B. R. Green, W. W. Parson, *Light-Harvesting Antennas in Photosynthesis*, Kluwer Academic, Dordrecht, **2003**, p. 544.
[2] S. Bahatyrova, R. N. Frese, C. A. Siebert, J. D. Olsen, K. O. van der Werf, R. van Grondelle, R. A. Niederman, P. A. Bullough, C. Otto, C. N. Hunter, *Nature* **2004**, *430*, 1058–1062.
[3] S. Scheuring, J. N. Sturgis, V. Prima, A. Bernadac, D. Lévy, J.-L. Rigaud, *Proc. Natl. Acad. Sci. USA* **2004**, *101*, 11293–11297.
[4] G. McDermott, S. M. Prince, A. A. Freer, A. M. Hawthornthwaite-Lawless, M. Z. Papiz, R. J. Cogdell, N. W. Isaacs, *Nature* **1995**, *374*, 517–521.
[5] A. W. Roszak, T. D. Howard, J. Southall, A. T. Gardiner, C. J. Law, N. W. Isaacs, R. J. Cogdell, *Science* **2003**, *302*, 1969–1972.
[6] J. Koepke, X. Hu, C. Muenke, K. Schulten, H. Michel, *Structure* **1996**, *4*, 581–597.
[7] X. Hu, T. Ritz, A. Damjanović, K. Schulten, *J. Phys. Chem. B* **1997**, *101*, 3854–3871.
[8] H. M. Wu, M. Ratsep, I. J. Lee, R. J. Cogdell, G. J. Small, *J. Phys. Chem. B* **1997**, *101*, 7654–7663.
[9] X. Hu, A. Damjanović, T. Ritz, K. Schulten, *Proc. Natl. Acad. Sci. USA* **1998**, *95*, 5935–5941.
[10] T. Hori, N. Aratani, A. Takagi, T. Matsumoto, T. Kawai, M.-C. Yoon, Z. S. Yoon, S. Cho, D. Kim, A. Osuka, *Chem. Eur. J.* **2006**, *12*, 1319–1327.
[11] M. C. Lensen, J. A. A. W. Elemans, S. J. T. van Dingenen, J. W. Gerritsen, S. Speller, A. E. Rowan, R. J. M. Nolte, *Chem. Eur. J.* **2007**, *13*, 7948–7956.
[12] C. A. Hunter, S. Tomas, *J. Am. Chem. Soc.* **2006**, *128*, 8975–8979.
[13] S. J. Lee, K. L. Mulfort, J. L. O'Donnell, X. Zuo, A. J. Goshe, P. J. Wesson, S. T. Nguyen, J. T. Hupp, D. M. Tiede, *Chem. Commun.* **2006**, 4581–4583.
[14] J. Aimi, Y. Nagamine, A. Tsuda, A. Muranaka, M. Uchiyama, T. Aida, *Angew. Chem.* **2008**, *120*, 5231–5234; *Angew. Chem. Int. Ed.* **2008**, *47*, 5153–5156.
[15] L. Flamigni, B. Ventura, A. I. Oliva, P. Ballester, *Chem. Eur. J.* **2008**, *14*, 4214–4224.
[16] R. F. Kelley, S. J. Lee, T. M. Wilson, Y. Nakamura, D. M. Tiede, A. Osuka, J. T. Hupp, M. R. Wasielewski, *J. Am. Chem. Soc.* **2008**, *130*, 4277–4284.
[17] S. J. Lee, K. L. Mulfort, X. Zuo, A. J. Goshe, P. J. Wesson, S. T. Nguyen, J. T. Hupp, D. M. Tiede, *J. Am. Chem. Soc.* **2008**, *130*, 836–838.
[18] S. Anderson, H. L. Anderson, J. K. M. Sanders, *Acc. Chem. Res.* **1993**, *26*, 469–475.
[19] A. K. Burrell, D. L. Officer, P. G. Plieger, D. C. W. Reid, *Chem. Rev.* **2001**, *101*, 2751–2796.
[20] L. Baldini, C. A. Hunter in *Advances in Inorganic Chemistry, Vol. 53* (Ed.: A. G. Sykes), **2002**, pp. 213–259.
[21] D. Holten, D. F. Bocian, J. S. Lindsey, *Acc. Chem. Res.* **2002**, *35*, 57–69.
[22] P. D. Harvey in *The Porphyrin Handbook, Vol. 18* (Eds.: K. M. Kadish, K. M. Smith, R. Guilard), Academic Press, New York, **2003**, pp. 63–250.
[23] K. Sugiura in *Topics in Current Chemistry, Vol. 228: Dendrimers V*, (Eds.: C. A. Schalley, F. Vögtle), Springer, Heidelberg, **2003**, pp. 3–14.
[24] M.-S. Choi, T. Yamazaki, I. Yamazaki, T. Aida, *Angew. Chem.* **2004**, *116*, 152–160; *Angew. Chem. Int. Ed.* **2004**, *43*, 150–158.
[25] H. Imahori, *J. Phys. Chem. B* **2004**, *108*, 6130–6143.
[26] D. Kim, A. Osuka, *Acc. Chem. Res.* **2004**, *37*, 735–745.
[27] A. Satake, Y. Kobuke, *Tetrahedron* **2005**, *61*, 13–41.
[28] C.-C. You, R. Dobrawa, C. R. Saha-Möller, F. Würthner in *Topics in Current Chemistry, Vol. 258: Supermolecular Dye Chemistry* (Ed.: F. Würthner), Springer, Heidelberg, **2005**, pp. 39–82.
[29] W.-D. Jang, N. Nishiyama, K. Kataoka, *Supramol. Chem.* **2007**, *19*, 309–314.
[30] S. Anderson, H. L. Anderson, J. K. M. Sanders, *Angew. Chem.* **1992**, *104*, 921–924; *Angew. Chem. Int. Ed. Engl.* **1992**, *31*, 907–910.
[31] J. K. M. Sanders in *Comprehensive Supramolecular Chemistry, Vol. 9* (Eds.: J. L. Atwood, J. E. D. Davies, D. D. MacNicol, F. Vögtle), Pergamon, Oxford, **1996**, pp. 131–164.
[32] M. Nakash, J. K. M. Sanders, *J. Org. Chem.* **2000**, *65*, 7266–7271.
[33] A. L. Kieran, A. D. Bond, A. M. Belenguer, J. K. M. Sanders, *Chem. Commun.* **2003**, 2674–2675.
[34] K. Y. Tomizaki, L. Yu, L. Wei, D. F. Bocian, J. S. Lindsey, *J. Org. Chem.* **2003**, *68*, 8199–8207.
[35] S. Rucareanu, A. Schuwey, A. Gossauer, *J. Am. Chem. Soc.* **2006**, *128*, 3396–3413.
[36] M. Hoffmann, C. J. Wilson, B. Odell, H. L. Anderson, *Angew. Chem.* **2007**, *119*, 3183–3186; *Angew. Chem. Int. Ed.* **2007**, *46*, 3122–3125.
[37] M. Hoffmann, J. Känbratt, M.-H. Chang, L. M. Herz, B. Albinsson, H. L. Anderson, *Angew. Chem.* **2008**, *120*, 5071–5074; *Angew. Chem. Int. Ed.* **2008**, *47*, 4993–4996.
[38] O. Mongin, A. Schuwey, M. A. Vallot, A. Gossauer, *Tetrahedron Lett.* **1999**, *40*, 8347–8350.
[39] X. Peng, N. Aratani, A. Takagi, T. Matsumoto, T. Kawai, I. W. Hwang, T. K. Ahn, D. Kim, A. Osuka, *J. Am. Chem. Soc.* **2004**, *126*, 4468–4469.
[40] Y. Nakamura, I.-W. Hwang, N. Aratani, T. K. Ahn, D. M. Ko, A. Takagi, T. Kawai, T. Matsumoto, D. Kim, A. Osuka, *J. Am. Chem. Soc.* **2005**, *127*, 236–246.
[41] T. Hori, X. Peng, N. Aratani, A. Takagi, T. Matsumoto, T. Kawai, Z. S. Yoon, M.-C. Yoon, J. Yang, D. Kim, A. Osuka, *Chem. Eur. J.* **2008**, *14*, 582–595.
[42] J. Yang, M. Park, Z. S. Yoon, T. Hori, X. Peng, N. Aratani, P. Dedecker, J.-i. Hotta, H. Uji-i, M. Sliwa, J. Hofkens, A. Osuka, D. Kim, *J. Am. Chem. Soc.* **2008**, *130*, 1879–1884.
[43] X. L. Chi, A. J. Guerin, R. A. Haycock, C. A. Hunter, L. D. Sarson, *J. Chem. Soc. Chem. Commun.* **1995**, 2563–2565.
[44] A. Tsuda, T. Nakamura, S. Sakamoto, K. Yamaguchi, A. Osuka, *Angew. Chem.* **2002**, *114*, 2941–2945; *Angew. Chem. Int. Ed.* **2002**, *41*, 2817–2821.
[45] R. Takahashi, Y. Kobuke, *J. Am. Chem. Soc.* **2003**, *125*, 2372–2373.
[46] C. Ikeda, A. Satake, Y. Kobuke, *Org. Lett.* **2003**, *5*, 4935–4938.
[47] I.-W. Hwang, M. Park, T. K. Ahn, Z. S. Yoon, D. M. Ko, D. Kim, F. Ito, Y. Ishibashi, S. R. Khan, Y. Nagasawa, H. Miyasaka, C. Ikeda, R. Takahashi, K. Ogawa, A. Satake, Y. Kobuke, *Chem. Eur. J.* **2005**, *11*, 3753–3761.
[48] R. A. Haycock, C. A. Hunter, D. A. James, U. Michelsen, L. R. Sutton, *Org. Lett.* **2000**, *2*, 2435–2438.
[49] O. Shoji, S. Okada, A. Satake, Y. Kobuke, *J. Am. Chem. Soc.* **2005**, *127*, 2201–2210.
[50] Y. Kuramochi, A. Satake, Y. Kobuke, *J. Am. Chem. Soc.* **2004**, *126*, 8668–8669.
[51] F. Hajjaj, Z. S. Yoon, M.-C. Yoon, J. Park, A. Satake, D. Kim, Y. Kobuke, *J. Am. Chem. Soc.* **2006**, *128*, 4612–4623.
[52] Y. Kuramochi, A. Satake, M. Itou, K. Ogawa, Y. Araki, O. Ito, Y. Kobuke, *Chem. Eur. J.* **2008**, *14*, 2827–2841.
[53] A. Ohashi, A. Satake, Y. Kobuke, *Bull. Chem. Soc. Jpn.* **2004**, *77*, 365–374.

[54] U. Michelsen, C. A. Hunter, *Angew. Chem.* **2000**, *112*, 780–783; *Angew. Chem. Int. Ed.* **2000**, *39*, 764–767.
[55] R. Takahashi, Y. Kobuke, *J. Org. Chem.* **2005**, *70*, 2745–2753.
[56] These calculation were carried out on WinMOPAC Ver. 3.9 (Fujitsu).
[57] W. Zhang, J. S. Moore, *J. Am. Chem. Soc.* **2005**, *127*, 11863–11870.
[58] M. Mammen, E. I. Shakhnovich, J. M. Deutch, G. M. Whitesides, *J. Org. Chem.* **1998**, *63*, 3821–3830.
[59] M. Kasha, *Radiat. Res.* **1963**, *20*, 55–70.
[60] A. Satake, Y. Kobuke, *Org. Biomol. Chem.* **2007**, *5*, 1679–1691.
[61] K. Mukai, S. Abe, H. Sumi, *J. Phys. Chem. B* **1999**, *103*, 6096–6102.
[62] L. R. Milgrom, P. J. F. Dempsey, G. Yahioglu, *Tetrahedron* **1996**, *52*, 9877–9890.

Received: July 19, 2008
Published online: October 16, 2008

